

## A Model Study on Understanding the Influence of Arabian Sea Mini Warm Pool on Monsoon Onset Vortex Formation

R. DEEPA,<sup>1</sup> C. GNANASEELAN,<sup>1</sup> M. DESHPANDE,<sup>1</sup> and P. S. SALVEKAR<sup>1</sup>

**Abstract**—The Arabian Sea Mini Warm Pool (MWP) is a zone of anomalously high Sea Surface Temperature (SST) in the Arabian Sea over which the monsoon onset vortex (OV) is believed to form. In the present study it is shown that this MWP is a key parameter in the development of the onset vortex. Atmospheric model experiments are carried out with and without MWP to understand the mechanisms for the formation of the OV. The model failed to simulate the OV with the cold SST advocating the importance of the MWP for the formation of the OV. The MWP is found to favor the formation of the onset vortex in the east central Arabian Sea by increasing the horizontal shear and decreasing the vertical wind shear.

### 1. Introduction

The north Indian Ocean (NIO) becomes the warmest area of the world oceans prior to the onset of southwest monsoon in late May or in early June with a huge warm pool (Sea Surface Temperature, SST > 28°C) (SEETARAMAYYA and MASTER 1984; JOSEPH 1990; VINAYACHANDRAN and SHETYE 1991; RAO and SIVAKUMAR 1999). The core of this warm pool lies (SST > 30.5°C) in the Lakshadweep Sea (SHENOI *et al.* 1999), the part of the southeast Arabian Sea (SEAS) that lies between the Indian peninsula and the Lakshadweep islands. The onset of summer monsoon over India is often, but not always, accompanied by the formation of an “onset vortex (OV)” (KRISHNAMURTI *et al.* 1981) in the SEAS and this suggests a possible link between the OV and the warm SEAS (JOSEPH 1990; RAO and SIVAKUMAR 1999; SHENOI *et al.* 1999). The OV, a low pressure system which forms over the east central Arabian Sea

(ECAS) on the leading edge of the monsoon current brings monsoon flow and sets the monsoon over the south peninsular India. It often deepens into a cyclonic storm, resulting in establishment of a region of convergence over the SEAS, which is followed by the strengthening of monsoon westerlies (ANANTHA-KRISHNAN 1964). In turn, the westerlies lead to sustained rainfall over Kerala, heralding the onset of the summer monsoon. The northward advancement of Indian summer monsoon is often associated with the northward (northwestward) propagation of OV. SHENOI *et al.* (1999) speculated that the Lakshadweep SST high probably provides a necessary, but not sufficient condition for the genesis of the monsoon OV. During winter there is no water (Fig. 1a) warmer than 28.5°C in the Mini Warm Pool (MWP) region. Warm water starts appearing in this region near the southwest coast of India during March. In May, the warm water reaches its maximum with a concentric region surrounded by water warmer than 30.5°C (SEETARAMAYYA and MASTER 1984; SHENOI *et al.* 1999; DEEPA *et al.* 2007) and it collapses with the onset of southwest monsoon. In addition to the large seasonal cycle, the MWP also shows a large interannual fluctuation in its areal extent and intensity.

SEETARAMAYYA and MASTER (1984) suggested that the anomalously high SSTs in the eastern Arabian Sea aided the development of the OV of 1979. KERSHAW (1988) using a numerical model studied the effect of SST anomaly on a prediction of the onset of the southwest monsoon over India. Recently, DEEPA *et al.* (2007) have studied the plausible reasons for the formation of the OV in the presence of the MWP. They have shown that though the ocean is fully co-operative with high thermal energy in the upper part, the OV does not form over the MWP unless the shear line forms along the northern flank of LLJ (at 850 hPa)

<sup>1</sup> Indian Institute of Tropical Meteorology, Pune 411008, India. E-mail: seelan@tropmet.res.in

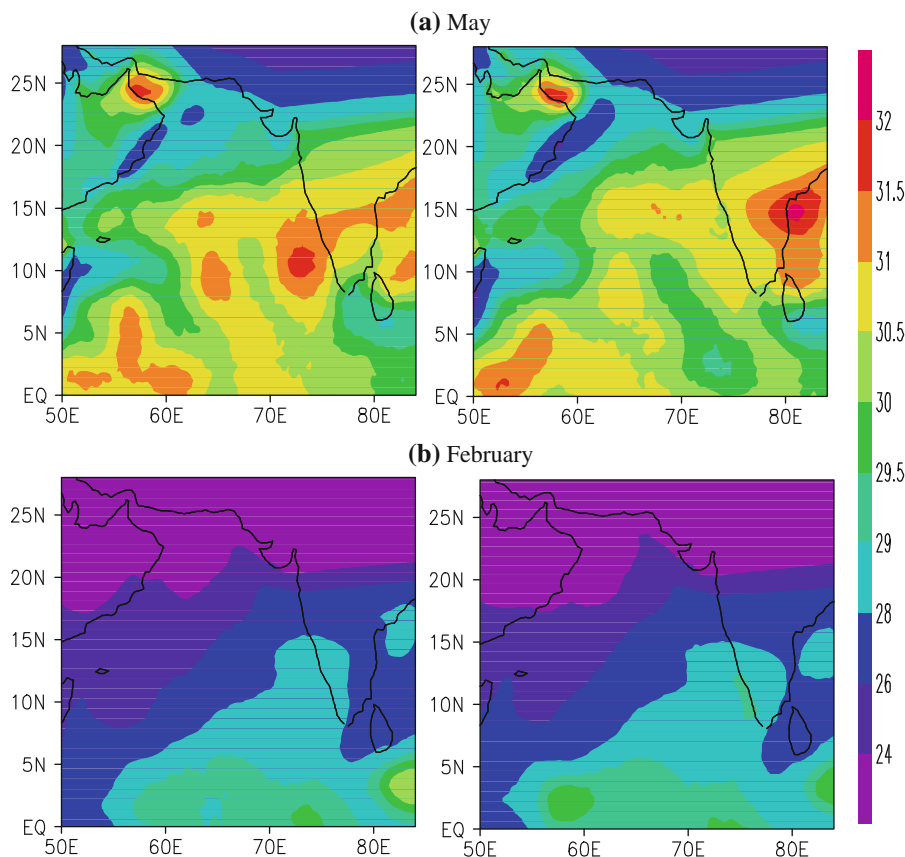


Figure 1

Sea Surface Temperature (SST) used as boundary condition for the model during **a** EXP1 (May SST) and **b** EXP2 (February SST)

near the west coast of India. VINAYACHANDRAN *et al.* (2007) have anticipated the necessity of model studies to establish a possible connection between the MWP and OV formation.

This paper is aimed to test the hypothesis proposed by the previous studies on the formation of the OV and understand the underlying mechanism for its formation. We tried to achieve this with a regional mesoscale atmospheric model. Several experiments are carried out with and without the MWP. This study also brings out the strong relationship possibly existing between the MWP, the Somali Low Level Jet (LLJ) and OV formation.

## 2. Data and Model

The atmospheric model used in this study is the Fifth Generation Pennsylvania State University/

National Center for Atmospheric Research (PSU/NCAR) Mesoscale Model (MM5) Version 3 (DUDHIA *et al.* 2004). The three dimensional simulations are carried out with two domains each with horizontal grid spacing of 90 and 30 km. Twenty-three sigma levels are used from the surface to 100 hPa. The cumulus parameterization by GRELL *et al.* (1994) and the mixed phase microphysics scheme are used for cloud physical processes. For initial and boundary conditions, National Centers for Environmental Prediction (NCEP) FNL reanalysis data and Real Time Global SST analysis from the NCEP are used. The model is integrated for 96 h from 00 UTC 19 May to 00 UTC 23 May 2001.

The MM5 model experiments were conducted with SST as a varying surface boundary condition with same initial atmospheric conditions from the NCEP. Several sensitivity experiments are carried out (with different SST conditions) to understand the role

of SST in the OV formation. Two such experiments have been explored in detail to understand the OV formation mechanism. In the first experiment (EXP1) the May SST has been provided as a boundary forcing whereas in the second experiment (EXP2) February SST has been given as surface boundary forcing (Fig. 1). In May the SEAS is occupied by an isotherm whose  $SST \geq 31.5^{\circ}\text{C}$ . It is surrounded by a  $31^{\circ}\text{C}$  isotherm. The region  $8\text{--}15^{\circ}\text{N}$ ,  $68\text{--}75^{\circ}\text{E}$  is engulfed by warm waters ( $SST \geq 30^{\circ}\text{C}$ ) in the Arabian Sea. The intrusion of cold waters from the Somali coast and southern tip of India can be noticed from the figure. The SST pattern during February is different from that of May. A  $28^{\circ}\text{C}$  isotherm is seen in the SEAS surrounded by a  $26^{\circ}\text{C}$  isotherm. Warm waters can be noticed near the equator associated with the northward march of the sun.

The identical model lateral boundary conditions are derived from the NCEP for both the experiments. It is found that the MM5 model has simulated the vortex with comparable intensity in the case of May SST boundary forcing. But the model failed to simulate the OV with February SST. This clearly highlights the importance of warm May SST in OV formation. It is important to note that the February SST was warm enough for convective activities especially in the southeast Arabian Sea. Several sensitivity experiments are conducted by varying the surface SST forcing to clearly understand the importance of MWP in OV formation. High SST (above  $30^{\circ}\text{C}$ ) is found to be the prerequisite for OV formation and intensification. Though the experiments with cooler SST (up to  $29^{\circ}\text{C}$ ) did show the formation of the OV but did not assist in the intensification.

### 3. Brief Description of the System

Development of an active equatorial trough in the NIO is witnessed from the beginning of the second half of May 2001. The optimum interpolation (OI) analysis showed the presence of a weak trough over the central Arabian Sea in the lower troposphere on 19 May with a cyclonic circulation at 500 hPa. Low level winds were southwesterly with speed of about 20 knots over the southwest Arabian Sea. A cyclonic

circulation developed at the leading edge of surging southwest monsoon flow in the lower troposphere over the central Arabian Sea which extended up to 500 hPa. Low level winds continued to be southwesterly and over 20 knots over southwest Arabian Sea. The circulation slowly moved eastwards and lay over ECAS on the morning of 20 May.

The relative vorticity field of 19 May also supports the above observations. Relative vorticity was positive and of the order of  $6\text{--}8 \times 10^{-5} \text{ s}^{-1}$  at 500 hPa over the central Arabian Sea and between 0 and  $2 \times 10^{-5} \text{ s}^{-1}$  at 850 hPa. Subsequently the positive vorticity field showed a gradual increase in the lower troposphere over the central Arabian Sea (the order of  $4\text{--}6 \times 10^{-5} \text{ s}^{-1}$ ) on 21 May at 850 hPa. The vertical wind shear between 200 and 850 hPa was generally small and of the order of 5–10 knots during the period 19–21 May which is considered favorable for cyclogenesis and further growth. Under these favorable conditions a depression formed in the ECAS on 21 May evening and was centered at  $13.5^{\circ}\text{N}$ ,  $69^{\circ}\text{E}$ . It intensified into a cyclonic storm and lay centered at  $14^{\circ}\text{N}$ ,  $71^{\circ}\text{E}$  on 22 May. This cyclonic storm over ECAS intensified into a severe cyclonic storm and then into a very severe cyclonic storm centered at  $15^{\circ}\text{N}$ ,  $71^{\circ}\text{E}$  on 23 May. The storm moved northwestward with its center at  $16.5^{\circ}\text{N}$ ,  $69.5^{\circ}\text{E}$  on 24 May. The very severe cyclonic storm weakened into a severe cyclonic storm on 26 May, and then moved northwards and lay centered at  $18^{\circ}\text{N}$ ,  $67.5^{\circ}\text{E}$  on 27 May (RSMC Report 2002).

## 4. Results and Discussion

### 4.1. Surface Pressure Variations from Model Simulations

Figure 2 represents the surface pressure variations from the model for 19–21 May 2001 (12 UTC). The upper panel represents the EXP1 case and the lower panel, the EXP2 case. The surface pressure starts decreasing at  $71^{\circ}\text{E}$ , between  $10$  and  $15^{\circ}\text{N}$  for the EXP1 case on 19 May (12 UTC). On the subsequent day the Arabian Sea is occupied by a low pressure area indicating the formation of a system. Finally, on

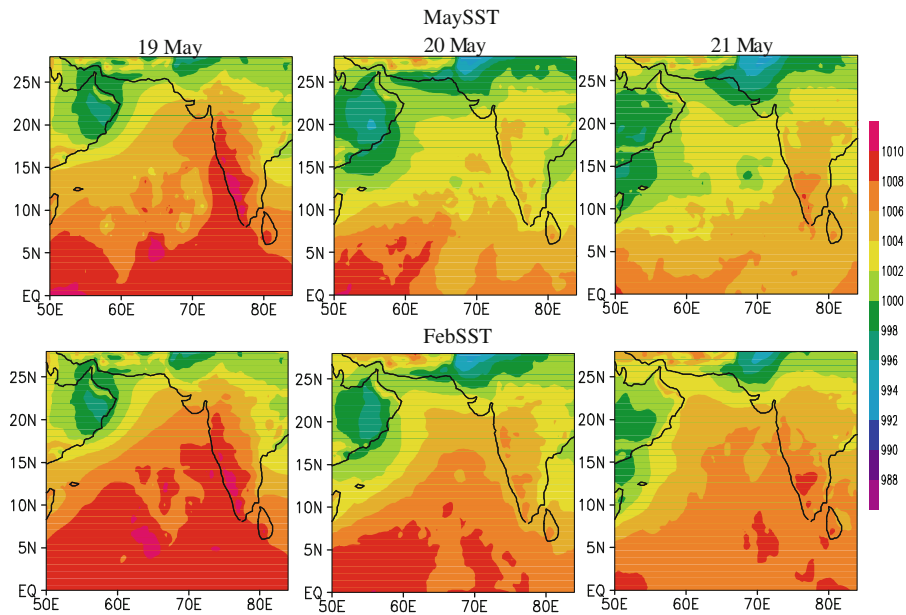


Figure 2  
Surface pressure variations from the model during EXP1 (May SST) and EXP2 (February SST)

21 May, a low pressure area of 998 hPa is noticed at  $12^{\circ}\text{N}$ ,  $71^{\circ}\text{E}$ , whereas the surface pressure did not show the formation of any system in EXP2. High pressure ridges can be noticed in the Arabian Sea.

#### 4.2. Wind Vector and Isotachs from Model Simulations

One of the most important features associated with the onset of monsoon is the establishment of the Somali Low Level Westerly Jet (hereafter LLJ) at 850 hPa over the Arabian Sea and the formation of a Tropical Easterly Jet in the upper troposphere. In 2001, a low pressure system formed one day before the onset of monsoon. This system in fact helped the northward advance of monsoon along the west coast of India.

In the experiment with the representation of MWP, hereafter EXP1, the 850 hPa LLJ reached the Somali coast on 19 May (Fig. 3a). On the subsequent day (20 May), the LLJ extended eastwards with a shear line at  $12^{\circ}\text{N}$ ,  $65^{\circ}\text{E}$  (Fig. 3b). The winds over Arabia were very strong and the northerlies strengthened and joined the low level flow. A decrease in wind speed is noticed north of  $15^{\circ}\text{N}$ . The wind intensified in the region south of  $10^{\circ}\text{N}$ , whereas

it weakened north of  $10^{\circ}\text{N}$  (Fig. 3c). The LLJ has further extended eastward and touched the west coast of India with a strong cyclonic circulation on its northern flank (Fig. 3d). While in the experiment without MWP, hereafter EXP2, the LLJ shows more or less the same intensity until 20 May and decays afterwards (Fig. 3d, right panel). The strength of the low level winds are very well captured in the EXP1 case and is comparable with the observations given by JTWC (UNISYS), but in the EXP2 case the winds are found to be very weak and the OV was absent in the model simulation.

In the EXP1 case, the 500 hPa wind field depicts the presence of an elongated trough region extending from the northern Arabian Sea westwards with strong northerlies and southwesterlies on both sides on day 1 of integration (Figures not shown). A weak low pressure area has formed along  $68^{\circ}\text{E}$  on the subsequent day and it moved eastwards with the eastward movement and intensification of the southwesterlies. The subtropical westerlies were pushed downward to become a part of the system circulation. While in the EXP2 case, on 20 May a trough was seen in between the northeasterlies and the westerlies. The trough has dissipated with the decay of low level westerlies on the subsequent days.

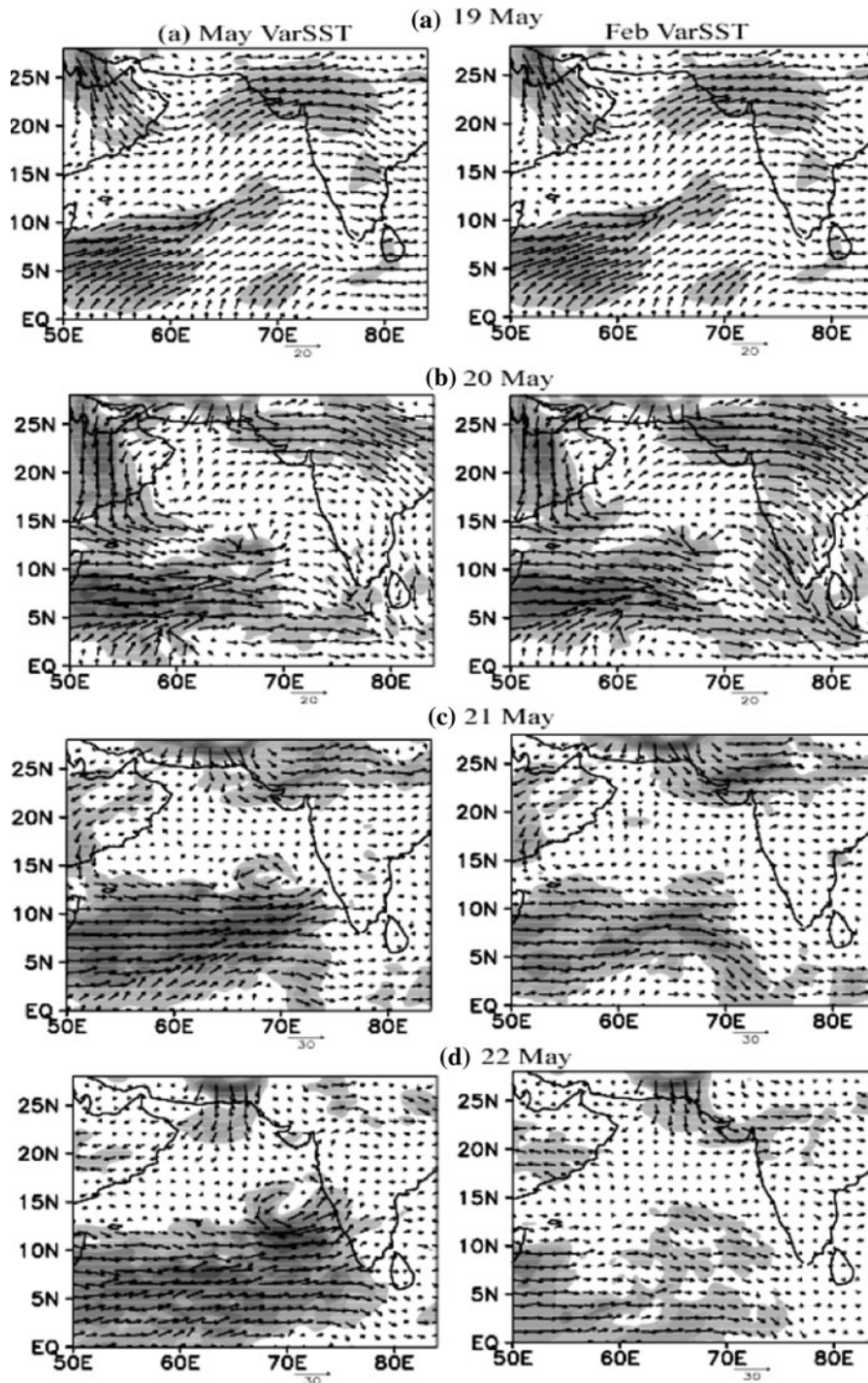


Figure 3

850 hPa circulation patterns for May SST (*left panel*) and February SST (*right panel*) from 19 May to 22 May 2001. The Low Level Jet is *shaded*

In the EXP1 case, upper level diffluence (200 hPa) is seen at 10°N, 60°E on 19 May (Figure not shown), whereas convergence and the formation of a low pressure area are observed at 850 hPa over the same region. The upper level anticyclonic circulation over Arabia is found to be strengthening and extending eastwards. The strength of anticyclonic circulation has reduced and the diffluence region has shifted eastwards near 70°E, and on 22 May the ECAS is fully dominated by upper level divergence, which is favorable for the formation of the system at lower levels. In the EXP2 case, the divergent circulation is present at 200 hPa until 20 May (15 UTC) and thereafter is dominated by the trough in the easterlies. So the subsequent convergence at 200 hPa and divergence at lower levels were unfavorable for the formation of the system.

From the analysis of the wind field, it is understood that the basic flow in which the incipient disturbance is embedded is an important environmental condition for storm genesis. It is noticed that the LLJ dissipated on the third day of integration (prediction) with cooler SST. LINDZEN and NIGAM (1987) has shown that the surface wind anomalies are entirely due to changes in the boundary layer virtual temperature distribution resulting from evaporative and sensible heat flux (SHF) anomalies associated with SST anomalies. The warm SST and the associated convection change the humidity and temperature profiles of the atmosphere, which then change the circulation pattern. The changes in deep convection act only indirectly to change the surface circulation by “venting” the boundary layer so as to reduce the hydrostatically induced horizontal pressure gradients. In spite of the favorable environmental factors, SST distribution is important for the formation and maintenance of the OV.

#### 4.3. Effect of Vertical Wind Shear on Onset Vortex Formation

The vertical wind shear between 200 and 850 hPa is represented in Fig. 4. A cyclonic circulation of low wind shear is prevalent at 16°N, 73°E surrounded by regions of high vertical wind shear for the EXP1 case (Fig. 4a). This cyclonic circulation is situated between two anticyclonic centers, one over Arabia

and the other over northeastern India. Both the anticyclones slowly subsided southwards on the subsequent days. The cyclonic circulation has moved over land by 21 May, whereas another anticyclonic circulation is seen between 12 and 16°N, 70°E (Fig. 4c). This anticyclonic circulation has moved eastwards and northwards to 16°N, 72°E. Finally on 22 May, the ECAS region adjacent to the west coast of India has become a very calm region, which is favorable for cyclogenesis and further growth, and a well marked low (Fig. 4d). In the EXP2 case, the anticyclone over northeastern India oscillated between 20°N and 12°N and an extended region of ridge is seen along 12°N. This has, in fact, prevented the formation of the system. On the subsequent days the anticyclonic wind shear over Arabia has reduced and the region north of 9°N is representative of low vertical wind shear. While for the EXP2 case, the wind shear was very low until 21 May 2001 and afterwards it started increasing.

The vertical shear has decreased in the EXP1 case compared to the EXP2 case. The MWPs affecting the vertical wind shear can be clearly inferred from the difference between model runs with MWP and without MWP. A negative vertical wind shear region is noticed over the OV. The combination of the MWP induced lower and upper tropospheric wind changes shows a large reduction in the model vertical wind shear. The gradient of SST directly influences the winds at upper levels through thermal wind relation. The vertical shear is associated with the removal of heat above the low-level disturbance by the wind relative to a moving disturbance (ventilation). Thus, the experiments suggest that MWP is important for reducing the vertical wind shear and favoring OV formation.

#### 4.4. Role of Thermodynamics in the Onset Vortex Initiation

The latent heat flux (LHF) distribution shows a high value for the EXP1 case (solid line) from 19 May onwards ( $>200 \text{ Wm}^{-2}$ ) indicating high values of flux transfer from the air–sea interface. While for the EXP2 case (dotted line) the flux transfer was very low, there was an initial increase from 19 May 00 to 12 UTC (nearly  $0\text{--}100 \text{ Wm}^{-2}$ ) and afterwards it

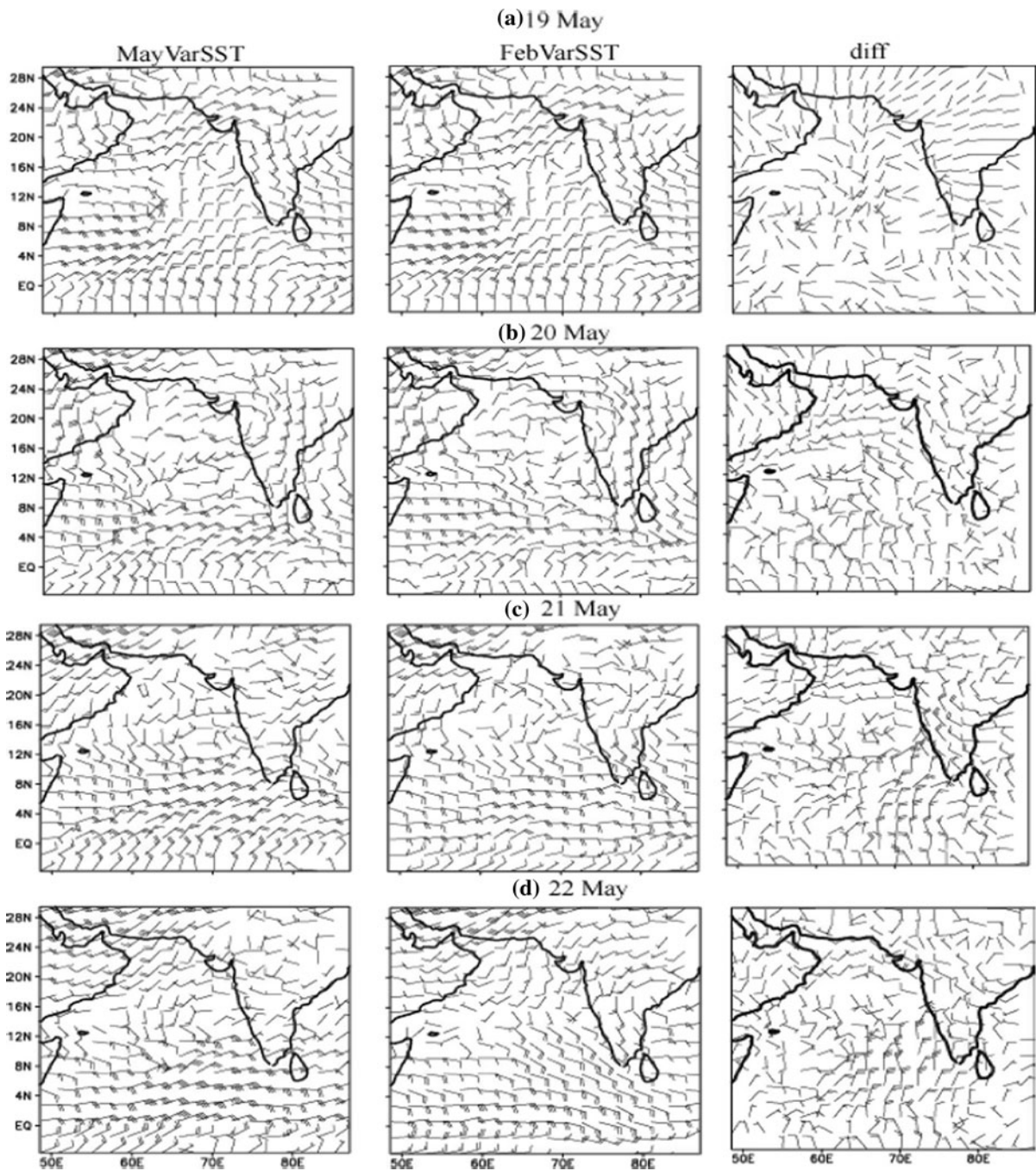


Figure 4

Vertical wind shear between 200 and 850 hPa for May SST (*left panel*), February SST (*middle panel*) and diff (May SST–February SST) (*right panel*)

remained more or less constant. On the incipient day of formation of a low, the LHF shows very high value of nearly  $380 \text{ Wm}^{-2}$  (Fig. 5a). The SHF also shows maxima on 21 May (Fig. 5b). The potential

temperature and equivalent potential temperature increased from 21 May onwards (Fig. 5c, d). Higher potential temperature represents warmer air while lower potential temperature represents colder air.

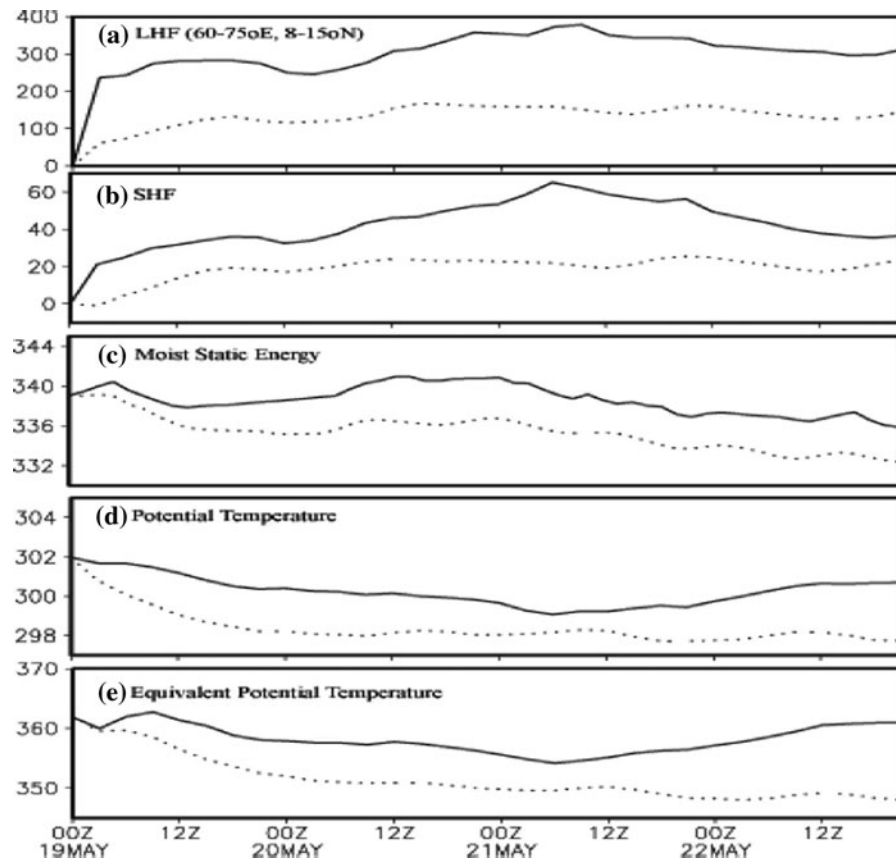


Figure 5

Time series of area averaged (65–75°E, 8–15°N). **a** Latent heat flux (LHF), **b** sensible heat flux (SHF), **c** moist static energy, **d** potential temperature and **e** equivalent potential temperature

Temperature (moisture) increase is responsible for the mid-level increase in equivalent potential temperature as the upper level warm, moist core and the low level vorticity intensify (TULEYA and KURIHARA 1982). The sudden change in equivalent potential temperature is due to the modification of the air temperature towards the saturation value and to the change in absolute humidity. The persistence of convection is an important factor for storm formation (CESELSKI 1974). The impact of convection can be noticed in the profile of potential temperature. While potential temperature can be used to compare temperatures at different elevations and the air parcels either raise or sink, equivalent potential temperature can be used to compare both moisture content and temperature of the air. The equivalent potential temperature is found by lowering an air parcel to the 1,000 mb level and releasing the latent heat in the

parcel. The lifting of a parcel from its original pressure level to the upper levels in the troposphere will release the latent heat of condensation and freezing of the air parcel. More the moisture the parcel contains, the more latent heat is released. Equivalent potential temperature is used operationally to map out the regions of most unstable and thus positively buoyant air. The equivalent potential temperature of an air parcel increases with increasing temperature and increasing moisture content. Therefore, in a region with adequate instability, areas of relatively high equivalent potential temperature are noticed. The moist static energy also showed high values from 19 May indicating more moisture content in the atmosphere. The cyclonic system has traveled from cold to warm waters eastward and then northwest and northwards. The disturbances propagate towards the northwest relative to the mean flow with

the most intense propagating the farthest north. CHANG and MADALA (1980) have observed that a tropical cyclone intensifies (decays) when encountering a broad area of warmer (colder) SST and

propagates faster (slower) ahead and to the right than a control experiment with uniform SST.

The virtual potential temperature distribution during EXP1 has shown subsidence along 65 and

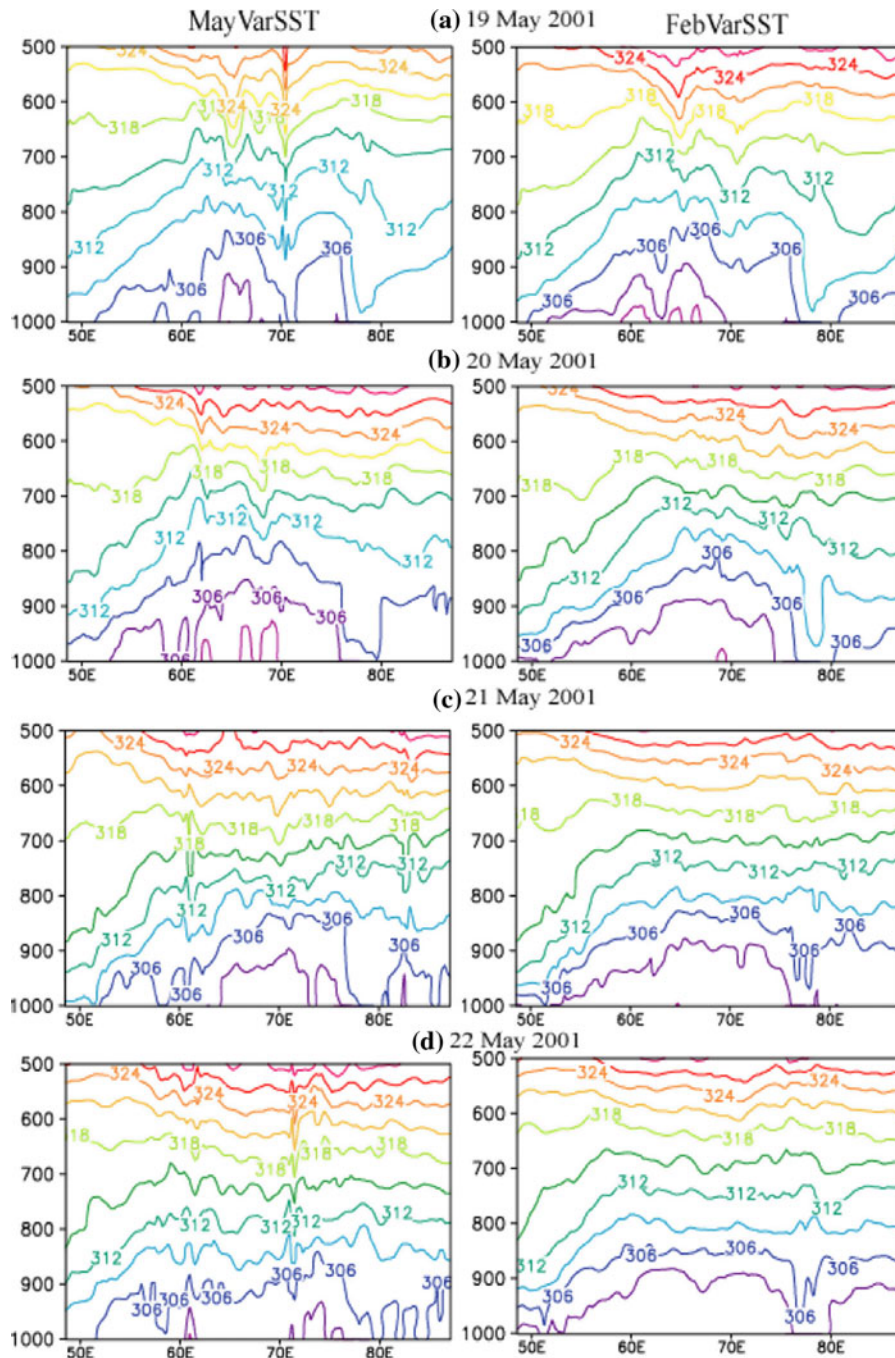


Figure 6  
Vertical profile of virtual potential temperature along 12°N for EXP1 (left panel) and EXP2 (right panel) cases

70°E (Fig. 6a). Along 65°E, subsidence is seen at lower levels and upward motions from the surface on 19 May 12 UTC (Fig. 6b). On 21 May (00 UTC) between 60 and 75°E, upward motions are present that extend up to 750 hPa level (Fig. 6e). Subsidence motions are, however, present above 750 hPa. The virtual potential temperature distribution on the incipient day of development of the vortex i.e. on

22 May shows upward motions up to 550 hPa level (Fig. 6g). On the subsequent day between 70 and 75°E, both subsidence and upward motions prevailed over the warm pool region. Thus, over the MWP region, both convergence and divergence motions are present. This strongly supports that the air–sea interface processes are responsible for the formation of the system. Whereas for EXP2, the deep

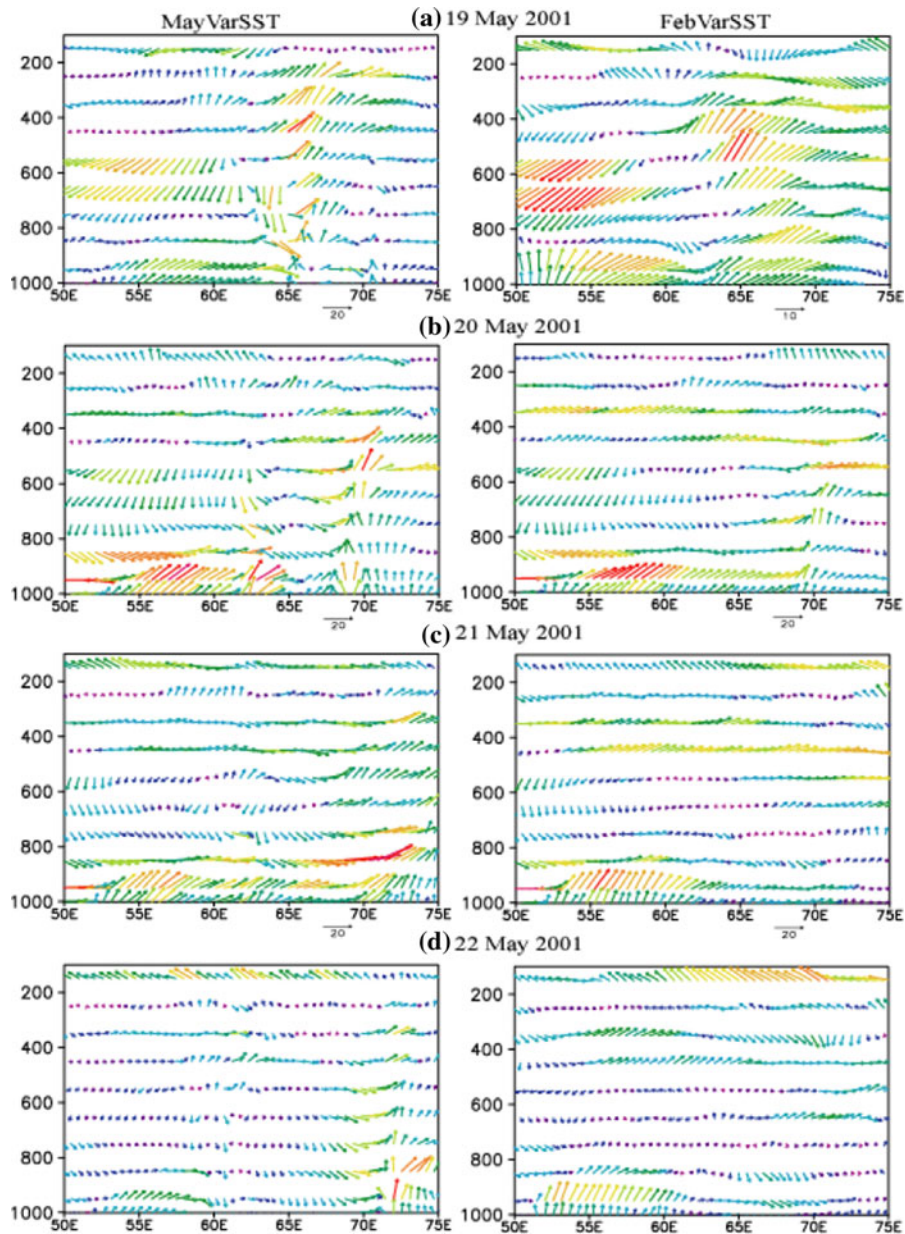


Figure 7  
Vertical profiles of wind vectors along 12°N for EXP1 and EXP2

convection is completely absent (Fig. 8, right panel). Weak upward motion is noticed only at the surface.

The vertical profile of wind along 12°N depicts strong winds between 65 and 75°E on the initial day of the prediction (Fig. 7b). The wind speed has

decreased on the second day of the prediction for the EXP2 (Fig. 7c). While on the third day of the prediction, the winds have changed direction from southwesterly to southerly in the region between 70 and 75°E for the EXP1 case, i.e., upward motion

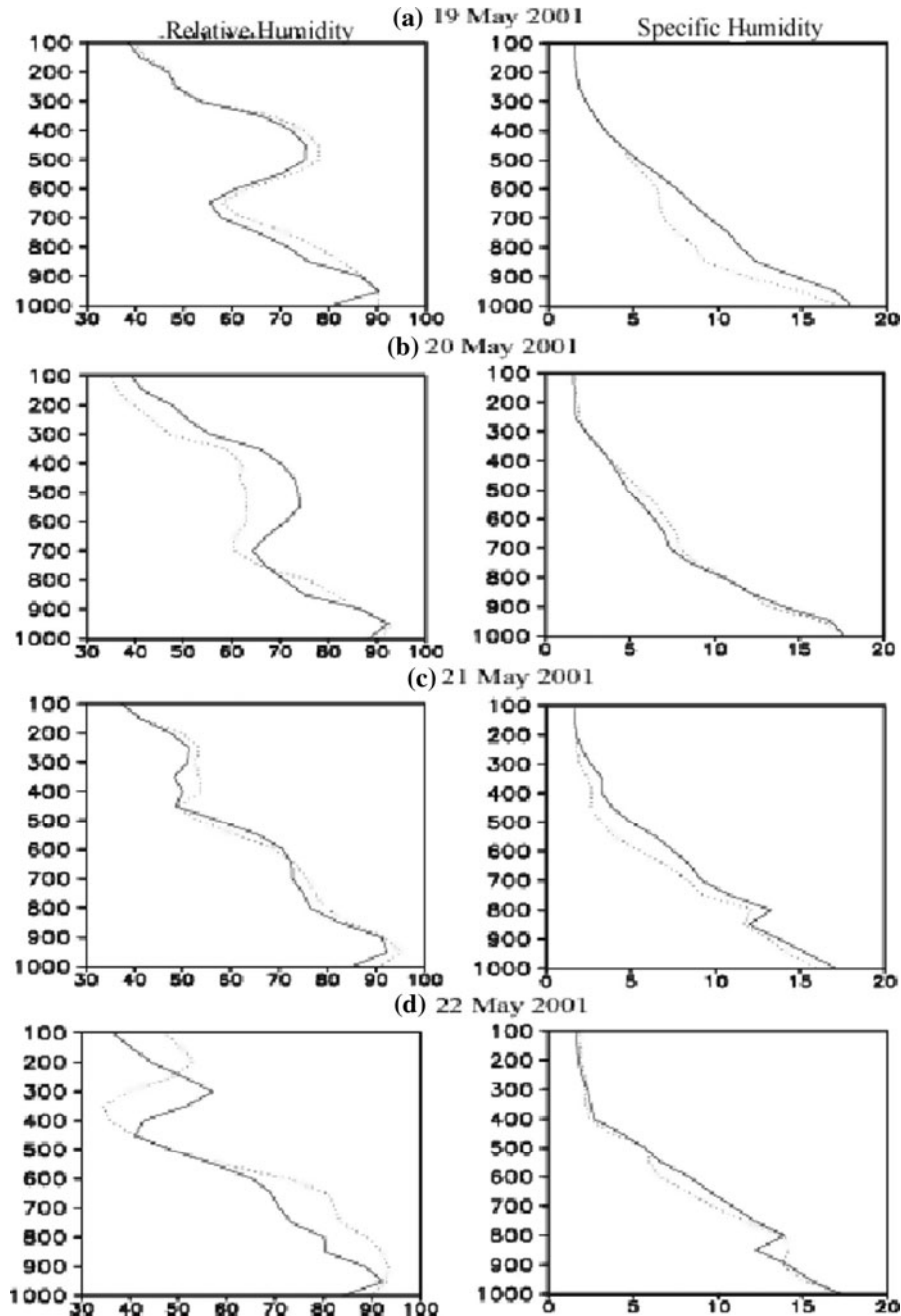


Figure 8

Vertical profiles of relative humidity (RH, solid lines) in % and specific humidity (g/kg, dotted lines) for EXP1 (left) and EXP2 (right) at 71°E, 12°N

persists over the warm pool region (Fig. 7d). For the EXP2 case, the winds have weakened at the surface between 65 and 75°E and increased towards the upper levels. This can be explained by the stability hypothesis of WALLACE (1989). According to this hypothesis, over warm SST (cold advection) the lower planetary boundary layer is turbulent and mixed. The unstable stratification over warm water mixes down momentum. The planetary boundary layer over cold SST (warm advection) is stably stratified. So the weak winds at the surface support shear in the region. The Arabian Sea warm pool is treated to be an area specific, which generally originates in the SEAS around Kerala latitude in the months March–April and slowly moves westward to the ECAS and lies between 10 and 15°N and east of 68°E. In May when the warm pool lies in the ECAS (i.e., lying between 10 and 15°N, 65–75°E) and the cold wind blows from west to east over the MWP and

the wind field accelerates on the western boundary of warm pool along 67°E, the air becomes warmer and the lower PBL becomes turbulent and well mixed. The winds will accelerate over the warm pool (WALLACE 1989; KRAUS and HANSON 1983; GILL 1980). Similarly, when the wind blows from warm waterside to cold waterside on the eastern boundary of the above warm pool, the air temperature decreases so that the PBL is less turbulent and weak mixing and the winds will decelerate on the windward side.

The vertical profile of meridional wind along 71°E and 12°N in EXP2 case shows much variation than the EXP1 case (Figure not shown). This is similar to the winter conditions. The profile of zonal wind for the EXP1 case shows weaker zonal vertical shear due to the reduced static stability over warm water. This reduced static stability intensifies the mixing leading to weaker zonal vertical shear. The 500 hPa relative humidity after 12 h of the prediction

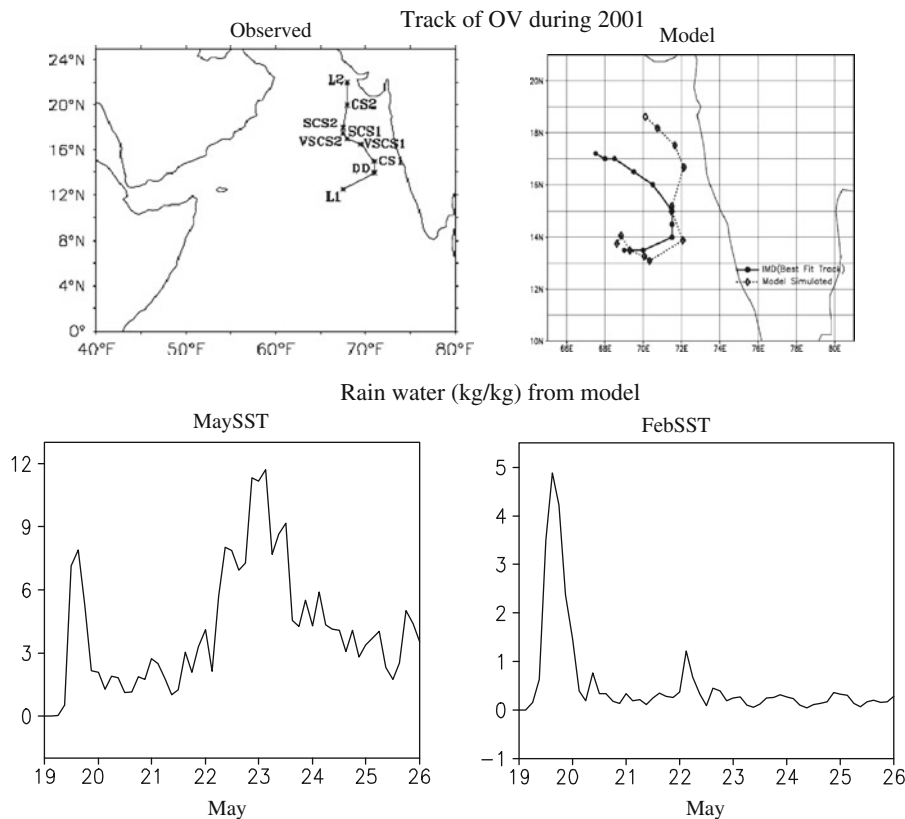


Figure 9

Tracks of the OV during 2001 (model and observed, upper panel) and model simulated rainwater averaged over 68–75°E, 8–15°N (cm/day) (lower panel)

represents 80% for the EXP2 case and 70% for the EXP1 case (Fig. 8a). On the first day of the prediction (Fig. 8b) the relative humidity of the EXP2 case decreased while that of the May SST case decreased. The meridional component showed maximum variation between the EXP1 and EXP2 cases. The u-profile also showed a somewhat similar trend. The minimum in southerly wind speed for the EXP2 case can be explained by the suppression of vertical mixing by high static stability over relatively cold waters. Another important point to be noticed is that an increase in relative humidity is noticed in the EXP2 case. As the air parcels cross from cold to warm waters, the atmospheric boundary layer undergoes a transition from a stable to an unstable regime. Such a transition should favor an increase in the surface wind speed through the enhanced downward flux of northward momentum from aloft by the increasingly vigorous, buoyancy-driven turbulence. Correspondingly, there is a decrease in relative humidity of the air at lower levels due to the enhanced downward mixing of drier air from aloft. The strong, northward directed pressure gradient force observed at the Earth's surface over the frontal zone should extend upward at least partway through the planetary boundary layer, accelerating the winds aloft. Horizontal divergence is indicative of subsidence aloft, which might be large enough to produce substantial vertical advection of momentum and potential temperature.

The track of the OV during 2001 is compared with the observed one. It is found that the model simulated track is comparable to the IMD best fit track (Fig. 9). The model simulated rain water (cm/day) for the EXP1 case shows two peaks, one just before the onset and the other one associated with the OV, whereas for the EXP2 case, only one peak is noticed as there is no formation of the system.

### 5. Summary

The sensitivity experiments using the atmospheric model (MM5) showed that warmer SST (greater than 30°C) is required for the formation of the OV and below which no OV forms or a very weak OV (much weaker than the observed OV) forms, regardless of

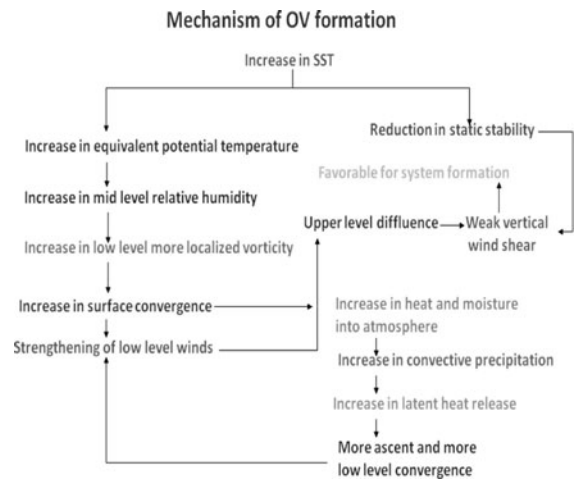


Figure 10  
Schematic of onset vortex formation

the favorable atmospheric conditions. The magnitude and gradient of SST in the Arabian Sea is important in OV genesis. In the month of May when the warm pool lies in the central Arabian Sea (10–15°N, 65–75°E), the cold wind blows from west to east over the MWP and the wind field accelerates on the western boundary of the warm pool along 67°E, the air becomes warmer, and the lower PBL is turbulent and mixed, and winds will accelerate over the warm water. Similarly, when the wind blows from warm water to cold water on the eastern boundary of the above warm pool, the air temperature decreases so that the PBL is less turbulent and the winds will decelerate on the windward side. Figure 10 presents the detailed schematic of the OV formation mechanism. An increase in SST leads to an increase in moisture at mid tropospheric levels. This will lead to an increase in equivalent potential temperature which in turn leads to a positive low level vorticity. This low level vorticity leads to more clouds and convective precipitation. Another consequence of an increase in SST is the reduction in static stability over warm water. These in turn lead to weaker zonal vertical shear that favors the formation of the system.

### Acknowledgments

The first author acknowledges CSIR, India for financial support. Thanks are also due to Director,

IITM and INCOIS, Hyderabad for support. The critical comments and very useful suggestions from the anonymous reviewers helped us to improve the manuscript considerably.

#### REFERENCES

- ANANTHAKRISHNAN R (1964) Tracks of storms and depressions in the Bay of Bengal and Arabian Sea. Technical report, India Meteorological Department, New Delhi, India.
- CESELSKI BF (1974): *Cumulus convection in weak and strong tropical disturbances*. J. Atmos. Sci. **31**: 1241–1255.
- CHANG SW and MADALA RV (1980) *Numerical simulation of the influence of sea surface temperature on translating tropical cyclones*. J. Atmos. Sci. **37**: 2617–2630.
- DEEPA R, SEETARAMAYYA P, NAGAR SG and GNANASEELAN C (2007) *On the plausible reasons for the formation of onset vortex in the presence of Arabian Sea mini warm pool*. Curr. Sci. **92**: 794–800.
- DUDHIA J, GILL D, MANNING K, WANG W and BRUYERE C (2004) PSU/NCAR Mesoscale Modeling System Tutorial Class Notes and User's Guide: MM5 Modeling System Version 3, National Center for Atmospheric Research, USA.
- GILL AE (1980) *Some simple solutions for heat induced tropical circulations*. Quart. J. Roy. Meteor. Soc. **106**: 447–462.
- GRELL GA, DUDHIA J, and STAUFFER D (1994) A description of the fifth generation Penn State/NCAR mesoscale model (MM5). NCAR Technical Note, NCAR TN-398-STR.
- JOSEPH PV (1990) *Warm pool over the Indian Ocean and monsoon onset*. Trop. Ocean–Atmos. Newslett. Winter, **1**–5.
- KERSHAW R (1988) *Effect of a sea surface temperature anomaly on a prediction of the onset of the southwest monsoon over India*. Quart. J. Roy. Meteor. Soc. **114**: 325–345.
- KRAUS EB and HANSON HP (1983) *Air–sea interaction as a propagator of equatorial ocean surface temperature anomalies*. J. Phys. Oceanogr. **13**: 130–138.
- KRISHNAMURTI TN, ARDANUY P, RAMANATHAN Y, and PASCH R (1981) *On the onset vortex of the summer monsoon*. Mon. Wea. Rev. **105**: 344–363.
- LINDZEN RS and NIGAM S (1987) *On the role of sea surface temperature gradients in forcing low-level winds and convergence in the tropics*. J. Atmos. Sci. **44**: 2418–2436.
- RAO RR, and SIVAKUMAR R (1999) *On the possible mechanisms of the evolution of the mini warm pool during the pre- summer monsoon season and the onset vortex in the southeastern Arabian Sea*. Quart. J. Roy. Meteor. Soc. **125**: 787–809.
- Report on cyclonic storms over the north Indian Ocean (2202) published by RSMC New Delhi, 2002.
- SEETARAMAYYA P and MASTER AH (1984) *Observed air–sea interface conditions and a monsoon depression during MONEX-79*. Arch Met Geoph. Biokl. **A33**: 61–67.
- SHENOI SSC, SHANKAR D and SHETYE SR (1999) *On the sea surface temperature high in the Lakshadweep Sea before the onset of the southwest monsoon*. J. Geophys. Res. **104**: 15,703–15, 712.
- TULEYA RE and KURIHARA Y (1982) *A note on the sea surface temperature sensitivity of a numerical model of tropical storm genesis*. J. Atmos. Sci. **110**: 2063–2069.
- VINAYACHANDRAN PN and SHETYE SR (1991) *The warm pool in the Indian Ocean*. Proc. Indian Acad. Sci., (Earth & Planetary Sci.) **100**: 165–175.
- VINAYACHANDRAN PN, SHANKAR D, KURIAN J, DURAND F and SHENOI SSC (2007) *Arabian Sea warm pool and monsoon onset vortex*. Curr. Sci. **93**: 203–214.
- WALLACE, J. M., T. P. MITCHELL, and C. DESER, 1989: *The influence of sea surface temperature variability upon surface wind in the eastern equatorial Pacific: Seasonal and interannual variability*. J. Climate **2**: 1492–1499.

(Received January 20, 2009, revised July 10, 2011, accepted August 10, 2011, Published online September 16, 2011)